WILEY | Hindawi

Research Article

Frequency Stability Enhancement of Microgrid Using Optimization Techniques-Based Adaptive Virtual Inertia Control

Philemon Yegon [1,2] and Mukhtiar Singh[1]

[1]Department of Electrical Engineering, Delhi Technological University, Delhi 110042, India
[2]Department of Electrical and Electronic Engineering, Kenyatta University, Nairobi 00100, Kenya

Correspondence should be addressed to Philemon Yegon; pkuruiphilemon@gmail.com

In recent years, a sharp increase in integration of renewable energy sources (RESs) in power system network has been observed. High penetration of RES interfaced with power electronics converters-inverters with reduced or no inherent inertia compromises modern power system's overall stability. Due to low inertia, voltage and frequency deviations far off the allowable threshold occur. To overcome this challenge, an adaptive inertia control strategy based on optimization technique is proposed. The improved particle swarm optimization (PSO) and genetic algorithm (GA) optimization techniques-based PID controller has been used to generate the appropriate virtual inertia coefficient for effective emulation of inertia in the presence of energy storage system. The conventional PSO suffers local optima stagnation, resulting in premature convergence during searching process in order to achieve global and local position. To address this issue, the velocity update equation was modified on inertia weight (w) using an additional exponential term with linear decreasing inertia weight PSO (LDIW-PSO). In this paper, exponential power is taken strategically instead of squaring it in order to reduce the number of iterations for faster convergence. Finally, a microgrid based on wind and solar energy is simulated using MATLAB/Simulink where three cases, 2% disturbance, 3% disturbance, and 4% disturbance, have been considered. Here, the evaluation of proposed system is carried out based on four main performance indices (ITAE, IAE, ISE, and ITSE). Furthermore, validation was done through hardware prototype to get experimental results in real time. The results from MATLAB simulation and experimental setup are in sync.

1. Introduction

In recent times, a drastic change in energy sector has been witnessed at global level. Due to ever-increasing number of consumers and the improvements in living standards among consumers, energy demand is escalating continuously. With these situations becoming compelling day by day, the conventional methods of power generation, i.e., fossil fuels, are not sustainable. Also, these traditional methods are not environmentally friendly. Coal produces greenhouse gas (GHG), which pollutes the surroundings and causes harm to the living organism in the area. They also emit carbon dioxide, which is a major cause of global warming. To meet this demand over a long period of time, RESs, for instance, wind, biomass, and solar, are now becoming popular. RESs have

a number of benefits as they are not destructive to environment and are relatively cheap. However, it is notable that they have low inertia and are intermittent in nature, nonlinear, and also uncertain [1]. There is a mismatch between generation and demand which causes an imbalance. The imbalance system makes introduced voltage and frequency deviations, which lead to a system's reduced reliability and resilience. It causes system collapse or even total blackout. In conventional power system, synchronous generators help to mitigate frequency deviation and RoCoF due to their ability to change speed when the system frequency changed. Kinetic energy is utilised (rotating mass) in traditional power system which is absent in the modern power system. Several power utility companies across the world invest millions of dollars annually to address frequency quality problem.

The increased penetration of RES has led to system instability due to intermittent feature of converter-inverter interface [2]. In addition, renewable energy sources, energy storage system, local loads, and power system applications are interconnected. Power electronics equipment lacks inherent inertia in comparison to synchronous machine in the traditional network. Due to large penetration of renewable energy sources in conventional power system network, considerable decrease in inertia is noted, causing frequency instability (frequency nadir and zenith and high rate of change of frequency). The frequency deviation is a notable problem in modern power system comprising power electronics-based energy harvesting from RES. To address the challenges associated with low inertia and frequency deviation, several methods have been reported previously. The use of wind turbine to generate inertia in microgrid had been proposed in [3]. Although this method seems to be very promising, the intermittency of wind speed and use of power electronics interface make it ineffective as an inertia source. Use of synchronous condenser has been widely used for inertia control but very expensive and not suitable for small systems like microgrid. Some of the researchers have also explored the use of ultracapacitors [4]. However, the regulation of high output current of ultra capacitors having high power density but low energy density is a major challenge. Similarly, the DC-link capacitor voltage control of grid-tied converter has been effectively used for inertia control. However, this method is not suitable for the interface of constant terminal voltage sources like batteries [5]. Use of DC-link capacitors; this method is effective in converters with variable voltages, however it can not be used for inertia control due to its limited energy storage capacity in microgrid [5]. Certain methods based on partial loading have been proposed to utilise the spare capacity of synchronous generator for inertial response. However, running a synchronous generator under partial loading conditions is highly inefficient and increases the per unit cost of electricity generation.

Recently, the concept of virtual synchronous machines (VSMs) emulated through power converter is gaining lot of popularity [6, 7]. Several research papers have looked into the effect of MGs and noninertia generation on the frequency reliability, resilience, and stability of bulk power systems [8–11]. Robust repetitive control (RC) is implemented in three-phase four-wire shunt active power filters (APFs) [12] for power quality in power system. In [14], a novel fractional-order controller was proposed for frequency regulation and real power fluctuation control but it did not explain how this controller is effective on offline microgrid and their cost implication if any. Furthermore, a well-structured frequency control system based on proportional, integral, and derivative (PID) controller optimized through metaheuristic techniques for microgrid system comprising wind, hydro, solar, diesel, and thermal systems was conducted to give ultimate quick control response to system disturbances [15, 16]. A malfunction lenient supervision for frequency and voltage was brought forward for a diesel engine machine applied on a microgrid. Nikhil Paliwal [17] in his paper implemented this control approach in a multi-source system (hydro power, gas turbine, and thermal plant), where the balance between power generation and demand as well as losses in microgrid has been achieved [18]. A similar control approach based on PID controller has been presented in [19] where the frequency control is implemented in hydro-wind hybrid system. The effectiveness of this method depends on the droop coefficient of synchronous generator [20]. Battery SOC time-varying properties are proposed in [21, 22] for the inertia enhancement.

Recently, a robust approach been presented by Shahryar Maleki and his colleagues in [23] where they employed linear matrix inequality method for optimal and robust control. However, the issues associated with the response time and parameter variations increase overall control complexities. Notably, it is clear from the given literature that there are technical gaps on design and analysis of virtual inertia control that need to be address in order to solve frequency deviation problem. The inertial response and damping coefficient are notable challenges in power electronic-interfaced microgrid.

In the proposed research work, adaptive virtual inertia control is proposed to overcome such a challenge of frequency instability using optimized PID controller-based energy storage system. In this novel concept, an improvised version of PSO and GA has been utilised to achieve optimal values for tuning of PID controller in low-inertia microgrid. Usually, a linear dynamic inertia weight updating equation is utilised for the enhanced PSO performance (LDIW-PSO) [24]. However, it suffers from the challenge of getting stuck into local optima during search space. In [25], a natural exponential with squared power term has been incorporated in weight updating equation. Although this approach is able to avoid local minima problem, it inherently suffers in terms of increased number of iterations which ultimately increases the convergence time. Moreover, the reduced values of w_{start} (0.6) and w_{end} (0.1) imply reducing viscosity as the search process is analogous to moving fluid. In this paper, natural exponential term is taken strategically without squaring it in order to reduce the number of iterations. Also, the higher values of w_{start} (0.9) and w_{end} (0.2) have been taken to reduce convergence time.

The key contribution of this paper is summarized here:

(i) Adaptive virtual inertia control is proposed to enhance frequency stability in a microgrid under different disturbances. During designing, performance index, RoCoF, frequency zenith, and frequency nadir have been considered to improve frequency response.

(ii) An improved particle swarm optimization algorithm has been implemented in this proposed control to deal with challenges of local optima and offer a balance distribution of particles between exploration and exploitation.

(iii) A brief comparison of frequency stability with traditional PSO, GA, and improved PSO under various operating conditions has been provided along with their procedural algorithm to demonstrate their performance.

(iv) The optimal gains obtained through proposed algorithm have been simulated on the given system and same have been validated through OPAL-RT supported hardware in loop in real time.

This paper is organized as follows. General introduction is given in Section 1. System description and control are presented in Section 2. Section 3 presents a brief description of optimization techniques applied, whereas Section 4 deals with simulation results and discussion. Section 5 represents experimental setup validation. Section 6 contains conclusion.

2. System Description and Control

The system under consideration is shown in Figure 1, where the model comprises both conventional sources of energy based on steam turbines for primary and secondary frequency control. Since RES is inertia-less, it needs to be regulated to avoid instability challenges. Therefore, solar and wind energy sources have also been considered for the formation of hybrid microgrid. The system is simulated under different generation and loading conditions while ensuring the frequency control within permissible limits. The mathematical modelling of all different power sources has been done and incorporated in the development of block diagram for the simulation purpose. The detailed mathematical formulation for different sources is as follows.

2.1. Modelling of Frequency Control System. In the first case, a model without virtual inertia is given as follows:

$$\Delta P_m(t) - \Delta P_L(t) = \frac{2Hd\Delta f(t)}{dt} + D\Delta f(t), \qquad (1)$$

where ΔP_m is power generation change by turbine, ΔP_L refers to change in power load, Δf refers to change in frequency, H is the inertia coefficient, and D is the damping constant. (1) is transformed to Laplace as

$$\Delta P_m(S) - \Delta P_L(S) = 2Hs\Delta f(S) + D\Delta f(S). \qquad (2)$$

(2) is represented in Figure 2.

Figure 3 shows the frequency deviation for both high inertia as well as low inertia system when put under certain disturbances. Here, it can be observed that in the absence of any regulating mechanism, the system droops, and it takes a long time to recover. Furthermore, the black solid line has small amplitude and it settled faster than the dotted red line. Therefore, it is always desirable to have a control system which could depict such excellent characteristics. Figure 3 shows hierarchical control structure with the secondary layer showing frequency restoration and control by stabilising the mismatch in load and generation.

The frequency change in a complete model is

$$\Delta f = \frac{\Delta P_m + \Delta P_W + \Delta P_{PV} + \Delta P_{VI} - \Delta P_L}{2Hs + D}, \qquad (3)$$

where

$$\Delta P_m(S) = \frac{1}{1 + sT_t}\Delta P_g(S),$$

$$\Delta P_g(S) = \frac{1}{1 + sT_g}\left(\Delta P_C(S) - \frac{1}{R}\Delta f(S)\right),$$

$$\Delta P_C(S) = \frac{Ks}{S}(\beta . \Delta f(S)), \qquad (4)$$

$$\Delta P_W(S) = \frac{1}{1 + sT_{WT}}\Delta P_{Wind}(S),$$

$$\Delta P_{PV}(S) = \frac{1}{1 + sT_{PV}}\Delta P_{Solar}(S),$$

where ΔP_C refers to ACE action change (signal), ΔP_P refers to change in power from primary control, ΔP_W refers to power change in wind system, ΔP_{Wind} refers to initial wind power change, ΔP_g refers to the power produced from the turbine, ΔP_{Solar} refers to the initial change in solar power, ΔP_{PV} refers to power produced by the solar system, ΔP_L refers to total change of load in the system, and ΔP_{VI} refers to change in virtual inertia power.

The variable loading, load shedding, and intermittent RES supply to the system cause fluctuation trend and hence result in poor frequency profile and interrupted energy supply to customer.

2.2. Control Description. The control part of any hybrid power system plays vital role in frequency stability, and it must be able to respond quickly to any kind of disturbances. It is always intended to have inertia control to respond first followed by primary and secondary control in case of a fault. Therefore, it is very necessary to emulate fast responding inertia control in the RES-based power system. Here, the damping coefficient plays vital role in minimizing the unwanted oscillations in the given system. A generalized virtual inertia control structure is shown in Figure 4 where the power disturbance may lead to frequency disturbance. Generally, a PID controller is included in a feedback closed-loop control mechanism [26]. PID transfer function comprises of first-order derivative and integral.

$$G_{Con}(s) = K_p + \frac{K_i}{s} + K_d s, \qquad (5)$$

where K_P, K_i, and K_d are proportional, integral, and derivative gains, respectively. Further, any power disturbance can be modelled as

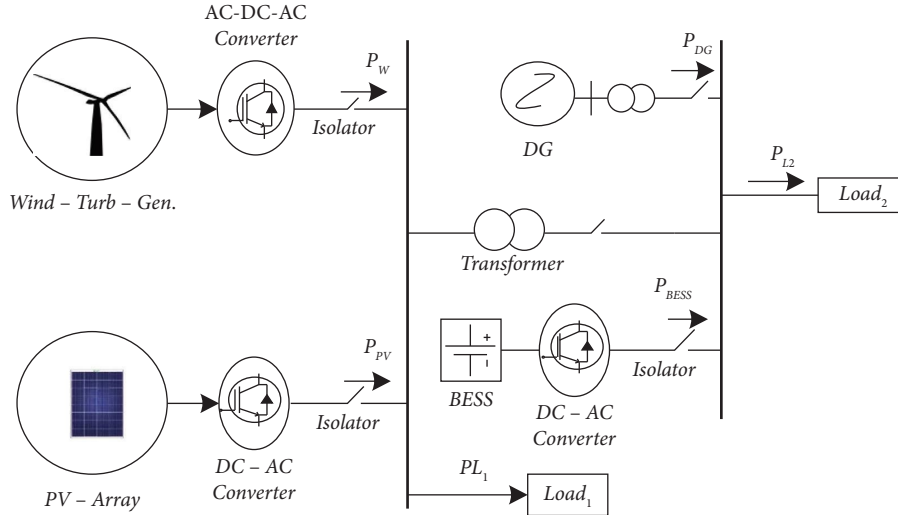$$\Delta P_{VI}(t) = \frac{\Delta f(K_{VI} + D_{VI})}{1 + sT_{ESS}}, \qquad (6)$$

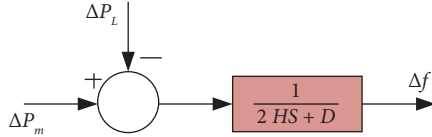FIGURE 1: The block diagram of converter interfaced in microgrid.
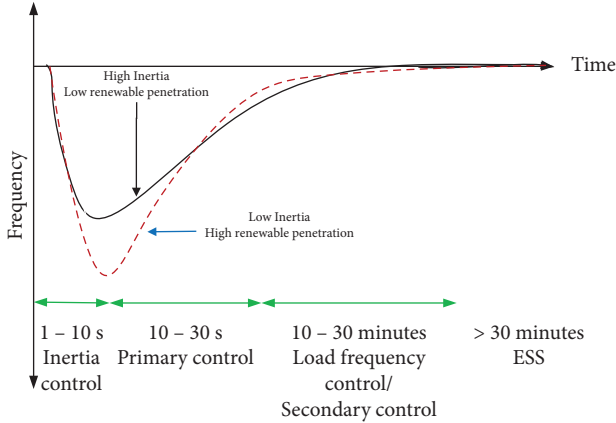

FIGURE 2: Frequency response model.

FIGURE 3: Response curve for inertial, primary, and secondary control.

where ΔP_{VI} is change in virtual inertia power input, K_{VI} is the virtual inertia coefficient, D_{VI} is the virtual damping coefficient, and T_{ESS} is the inverter-based energy storage system (ESS) time constant.

2.3. System Parameters. In this paper, the parameters used for modelling and frequency regulation have been adopted from [27] and are also enumerated in Table 1.

3. Optimization Techniques Applied

The control performance of the given system depends on the tuning of PID regulator. Under the normal circumstances,

a generalized PID may exhibit satisfactory performance. However, its performance starts deteriorating under the dynamic load conditions/intermittent power generation from RES. Therefore, it makes it necessary to search for the optimal gains of PID regulator which may perform under all such dynamically operating conditions. An improvised form of PSO and GA has been utilised to obtain the optimized value of PID gains for virtual inertia control under the different operating conditions. For this purpose, the control block diagram as shown in Figure 5 has been modified by incorporating frequency disturbance signal in the tuning of PID controller using the improvised form of PSO and GA optimization algorithms. The whole system is simulated in MATLAB/Simulink as per the block diagram shown in Figure 6. The simulation study is carried out for three different cases while considering the different levels of disturbances, either from the load or renewable power sources being intermittent in nature. In Case 1, a disturbance of 2% was considered at $t = 0.2s$. In the second case, a disturbance of 3% occurred at $t = 2.2s$ and finally a third disturbance of 4% is introduced at $t = 4.5s$. All the 3 cases were considered using both optimization techniques.

3.1. Particle Swarm Optimization (PSO). Particle swarm optimization (PSO) was introduced in 1995 by James Kennedy and Russel C. Eberhart [28] inspired by the social behaviour of animals like flock of birds and the school of fish. It is a simple but powerful optimization algorithm; it is an effective technique utilised in optimization challenges. This technique has been applied in a variety of applications. It has various advantages, for instance, efficiency in mathematical computation, simple to implement, robust, and stable convergence characteristics [29], and it can also be used in online optimization due to its efficiency and simplicity [30].

The conventional particle swarm optimization is a design based on the behaviour of a swarm of birds in search of food location [28]. The position location and speed of each
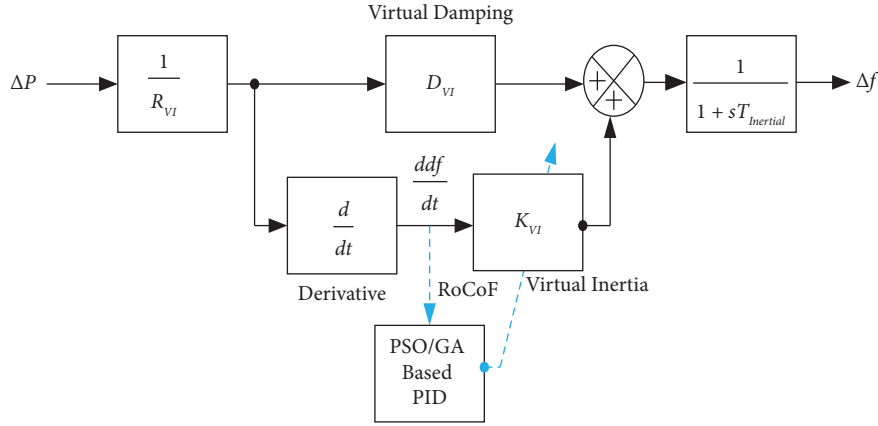
FIGURE 4: Virtual inertia control structure.

TABLE 1: System parameter values.

Description	Symbol	Value
Turbine time coefficient	T_{urbine}	0.5 s
Governor time coefficient	T_g	0.2 s
Generator inertia coefficient	H	5 s
Governor speed regulation	R per min	0.05
Damping coefficient	D	0.8

particle are located by the following equation; the best local position (P_i) and global best (G_i):

$$X_i^{t+1} = X_i^t + V_i^{t+1},$$
$$V_i^{t+1} = wV_i^t + c_1 r_1 \left(P_i^t - X_i^t\right) + c_2 r_2 \left(G_i^t - X_i^t\right), \quad (7)$$

where r_1 and r_2 are random values in the range of [0, 1], c_1 and c_2 are social and cognitive constants, w is the inertia weighting function, wV_i^t is inertia, $c_1 r_1 (P_i^t - X_i^t)$ is the cognitive component, and $c_2 r_2 (G_i^t - X_i^t)$ is the social component.

w is inertia weight which is very critical for the fast convergence of optimization process. A very effective approach based on linear decreasing inertia weight PSO has been presented in [24] to manipulate the inertia weight and update it dynamically as represented by equation given below:

$$w = \left(w_{start} - w_{end}\right) \times \left(\frac{T_{max} - t}{T_{max}}\right) + w_{end}, \quad (8)$$

where w_{start} is the initial value of inertia weight, w_{end} is the final value of inertia, and T_{max} refers to maximum iterations.

The linear dynamic inertia weight-PSO (LDIW-PSO) faced challenge of falling into local optimum during the searching process. Moreover, the performance of optimization engine is heavily dependent on initial and end values of inertia constant where the too small or too much higher values may increase no. of iterations as well as convergence time. To overcome this issue, natural exponential is multiplied with w_{end} to enhance velocity-updating equation. Similarly, the authors of [25] have included a square of exponential which further increases the computational burden. Therefore, in order to reduce the computational

burden without compromising in performance, an exponential term with suitable value of T_{max} has been included in weight updating matrix such that the overall convergence time reduces with reduced no. of iterations [25, 31]. The modified equation is as given below:

$$w = \left(w_{start} - w_{end}\right) \times \left(\frac{T_{max} - t}{T_{max}}\right) + w_{end} \times e^{-t/(T_{max}/10)}, \quad (9)$$

where $w_{start} = 0.9$ and $w_{end} = 0.2$.

Figure 7 illustrates that MPSO converged faster than LDIW-PSO. It shows better performance.

3.2. Genetic Algorithm (GA).

To improve system response of inertia-less microgrid, GA has been used to optimize PID parameters so that it effectively and efficiently gives optimal values. With the repetitive loops, chromosome population is iterated; in this case, each iteration is considered as a generation. The genetic material operators are concern with selection, crossover, and mutation to form a new cluster [32]. There is an objective function for each generation. Charles Darwin's selection criteria are applied, and Darwin's fitness and the struggle for survival strategy are used [33].

The probability equation is

$$p(\eta, t) = M \frac{p(\eta, t-1) f(\eta)}{\sum f(H)}, \quad (10)$$

where p is probability, η refers to gene, t refers to time, M refers to population, $f(\eta)$ refers to fitness value gene, and $\sum f(H)$ refers to sum of fitness value of all populations. GA is applied, and the boundary values of PID controller gains K_p, K_i, and K_d are obtained through the GA optimization process. The algorithm shown in Figures 8 and 9 depicts step by step procedure on how improved PSO and GA optimization works.

3.3. Formulation of Four Performance Indices (PIs).

In this research paper, improved PSO and GA are applied to minimize the error in performance index. The error, that is, the deviation in frequency should be as minimal as possible.
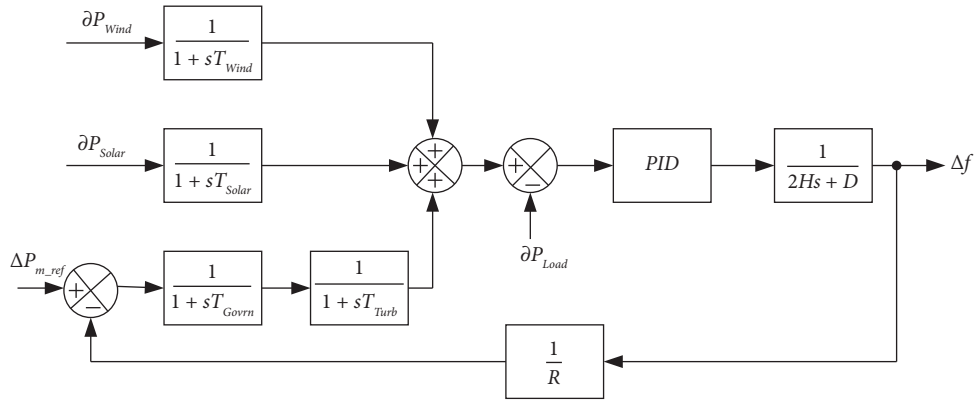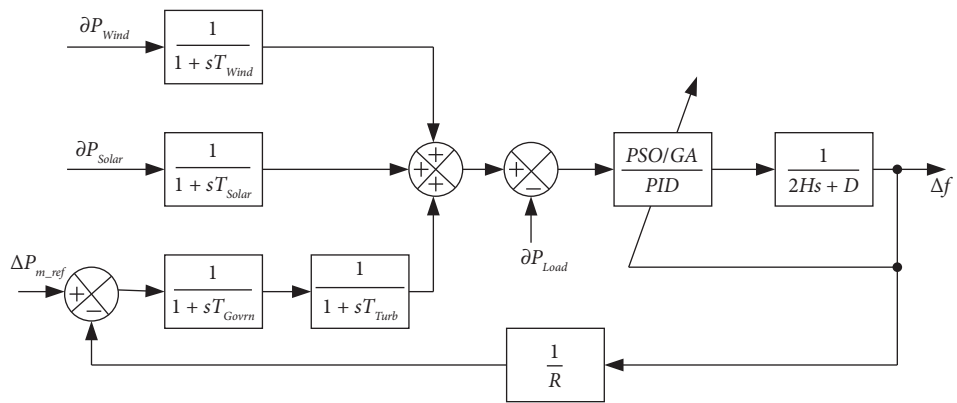
Figure 5: Microgrid control with PID.
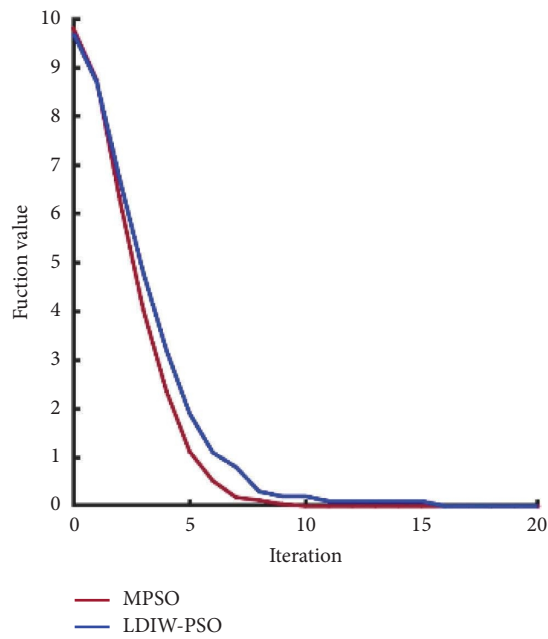

Figure 6: Designed proposed layout.

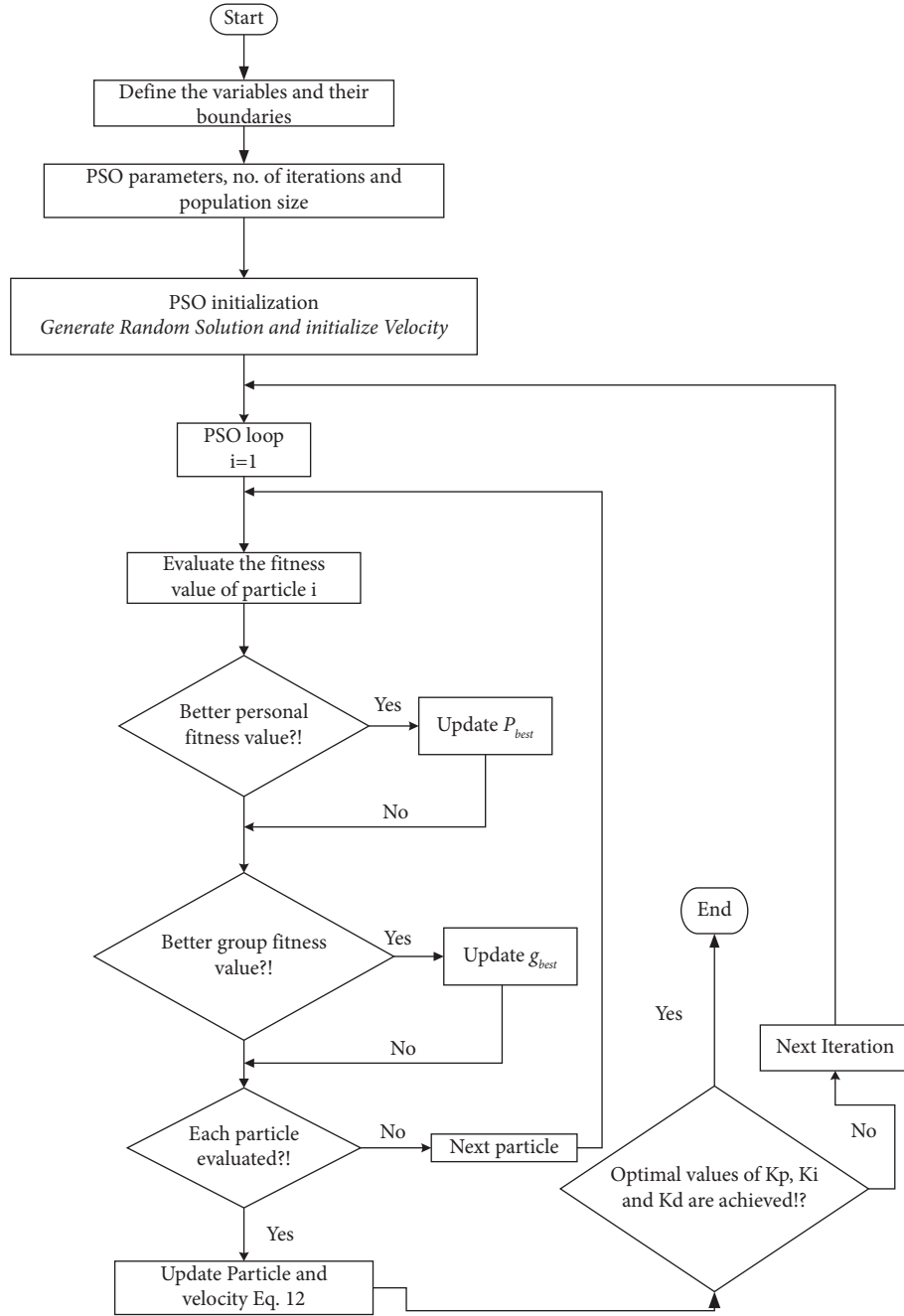Figure 7: Comparison of MPSO and LDIW-PSO.

Figure 8: Particle swarm optimization (PSO) flowchart.

During this research, four performance indices were considered: integral time-weighted absolute error (ITAE), integral absolute error (IAE), integral time square error (ITSE), and integral square error (ISE). The following objective functions have been mathematically formulated.

Integral time-weighted absolute error (ITAE):

$$ITAE = \int_0^{t_{Sim}} t|\Delta f|dt. \quad (11)$$

Integral absolute error (IAE):

$$IAE = \int_0^{t_{Sim}} |\Delta f|dt. \quad (12)$$

Integral square error (ISE):

$$ISE = \int_0^{t_{Sim}} |\Delta f^2|dt. \quad (13)$$

Integral time square error (ITSE):

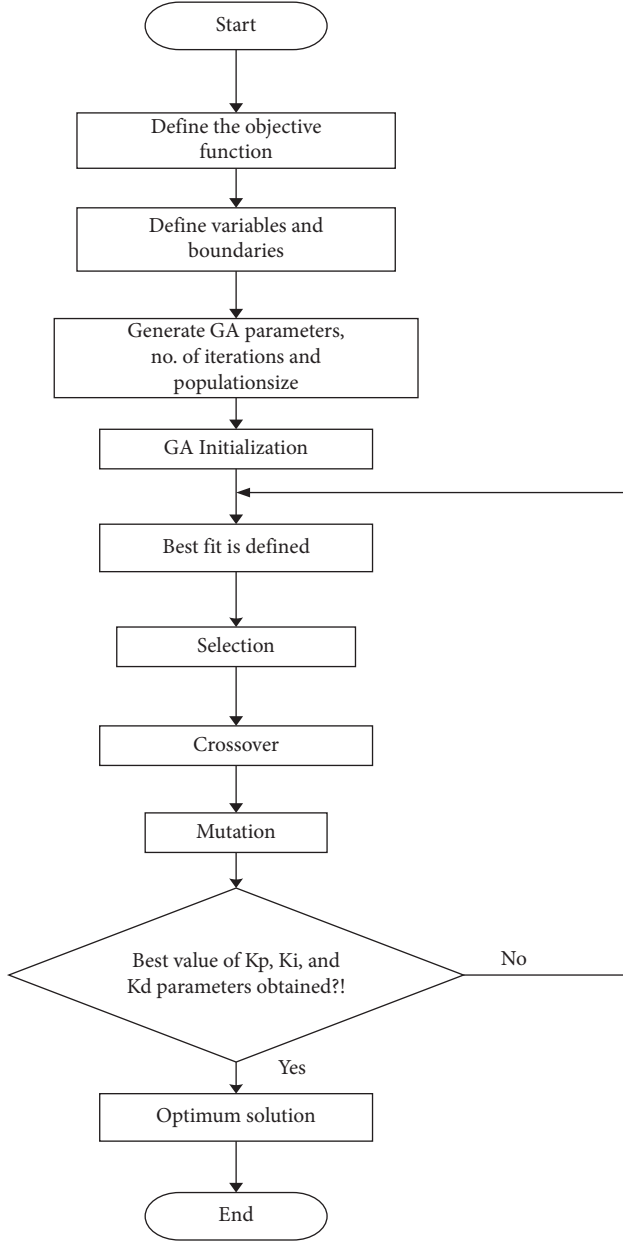$$ITSE = \int_0^{t_{Sim}} t|\Delta f^2|dt. \quad (14)$$

FIGURE 9: Genetic algorithm (GA) flowchart.

The deviation in frequency (Δf) is due to perturbation in power system due to intermittent power supply and nonlinear loads. Time range for simulation is denoted as t_{Sim}. Minimize P.I. subject to equation (15). Here , the selected range of PID parameters gains K_p, K_i, and K_d are considered.

$$
\left. \begin{array}{l}
K_{p\mathrm{Upper}} \geq K_p \geq K_{p\mathrm{Lower}}, \\
K_{i\mathrm{Upper}} \geq K_i \geq K_{i\mathrm{Lower}}, \\
K_{d\mathrm{Upper}} \geq K_d \geq K_{d\mathrm{Lower}},
\end{array} \right\}
\tag{15}
$$

where the population size, iterations, and boundary size taken are provided in Tables 2 and 3.

TABLE 2: PSO and GA elements.

Elements	Data
Population size	100
Maximum iteration	50

TABLE 3: PSO and GA boundary condition.

Parameters	Lower boundary	Upper boundary
K_P	0	1000
K_I	0	1000
K_D	0	1000

4. Simulation Results and Discussion

The simulation of the 250 MW system with RES penetration is shown in Figure 1. It consists of DG 200 MW, solar power plant 15 MW, wind power plant 25 MW, 10 MW of BESS, residential load of 5 MW, and 10 MW industrial load [34, 35] which are incorporated with the proposed controller. The optimal gains obtained from the two techniques are tabulated in Table 4. Here, all the four performance indices were considered for each case.

Series of simulations were conducted in MATLAB environment to obtain optimal parameters values for different algorithms. Given below are algorithms for improved PSO and GA showing parameter settings, initialization, termination, and fitness function.

Improved PSO has a population size of 100, maximum number of iterations 50, minimum fitness of 0.0001, maximum and minimum allowable velocities $V_{\mathrm{max}} = 1$; $V_{\mathrm{min}} = -1$, acceleration constants $C_1 = 2$; $C_2 = 2$, and the other parameter is inertia weight which has been modified as discussed earlier in Section 3.1.

Similarly, the population size for GA is 100 and the number of iterations (generations) is 50. The cross probability is 0.8, and cross mutation is 0.1. In Figures 10 and 11, optimal individual fitness-based improved PSO and GA are illustrated with the four performance indices. Optimization curves for the PID parameters are shown in Figure 12; each curve shows the optimal value of each constant.

The optimization techniques used above are able to minimize error and their evaluation is carried out on the basis of four main performance indices, where the settling time, undershoot, overshoot, and oscillation got improved drastically. The RoCoF and deviation in frequency are brought to steady state within few milliseconds unlike the conventional rotational mass of synchronous machines which takes up to 10 seconds to settle down. The response is very fast and comes in effect well before the primary response which sets in between $30 s$ and $30 m$ and the secondary frequency control which sets in after the 30th minute to shed off the loads or to operate the protective mechanism. The simulation study is carried out under three different operating conditions, where Case 1 with 2% disturbance, Case 2 with 3% disturbance, and Case 3 with 4% disturbance are considered.

TABLE 4: PSO and GA-optimized PID gains with performance indices.

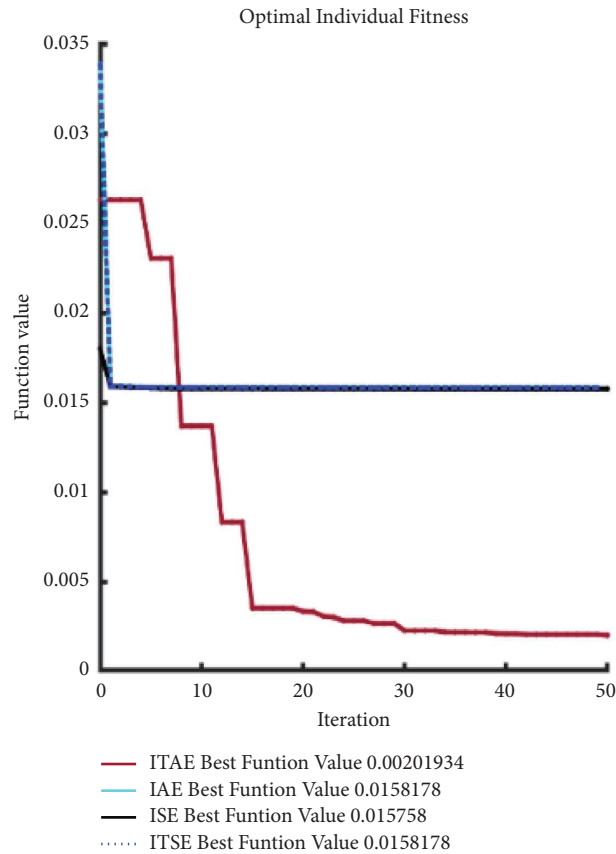| Parameters	PSO and GA-optimized values							
	ITAE		IAE		ISE		ITSE	
	PSO	GA	PSO	GA	PSO	GA	PSO	GA
K_P	1000	913.6278	1000	970.5514	1000	810.4577	1000	760.6385
K_I	4.4809	1.3339	2.1039	243.1919	0.6580	0.0233	2.1041	2.7500
K_D	0	1	0	0.7023	0	1.2251	0	8.1265

FIGURE 10: PSO-based optimization curve.

Case 1. 2% disturbance: Initially, the system is stable with the frequency of 50Hz for the first 0.2seconds, and then an abrupt load demand of 5MW is introduced which results in frequency disturbance. The frequency oscillations take almost 20.734ms to damp out and system is restored again to stable operation with 50 Hz frequency while feeding a load of 245 MW.

Case 2. 3% disturbance: After 2.2seconds, a RES starts supplying the power of 7.5MW which results in power and frequency oscillations. It takes almost 23.645ms to damp out the oscillations. Finally, the frequency is again restored to its nominal value while feeding the load of 252.5 MW.

Case 3. 4% disturbance: At 4.5 seconds, another disturbance occurred with a reduced load demand of 10 MW. This results in the higher amplitude of frequency and power oscillations and it takes almost 24.505ms to damp out these oscillations. Again, the frequency gets settled down to its nominal value with overall system load of 242.5 MW.
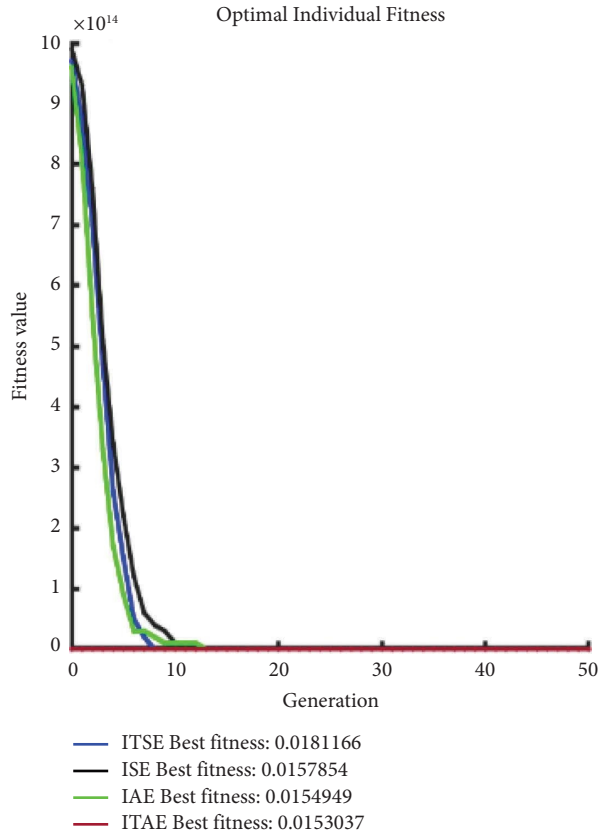
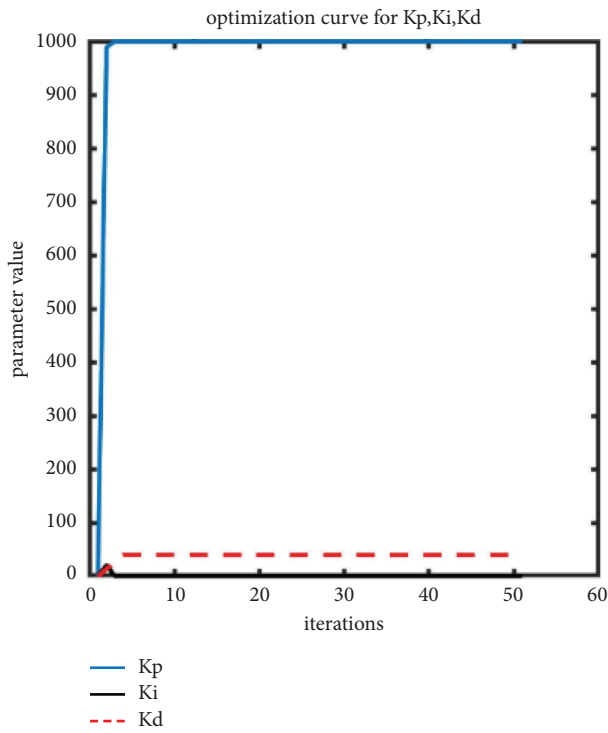Figure 11: GA-based fitness curve.

Figure 12: Optimization curve for K_P, K_i, and K_d.

FIGURE 13: Response curves for change in frequency, frequency, change in power, and power optimized by improved PSO and GA-based P.I-ITAE.

FIGURE 14: Response curves for change in frequency, frequency, change in power, and power optimized by improved PSO and GA-based P.I-IAE.
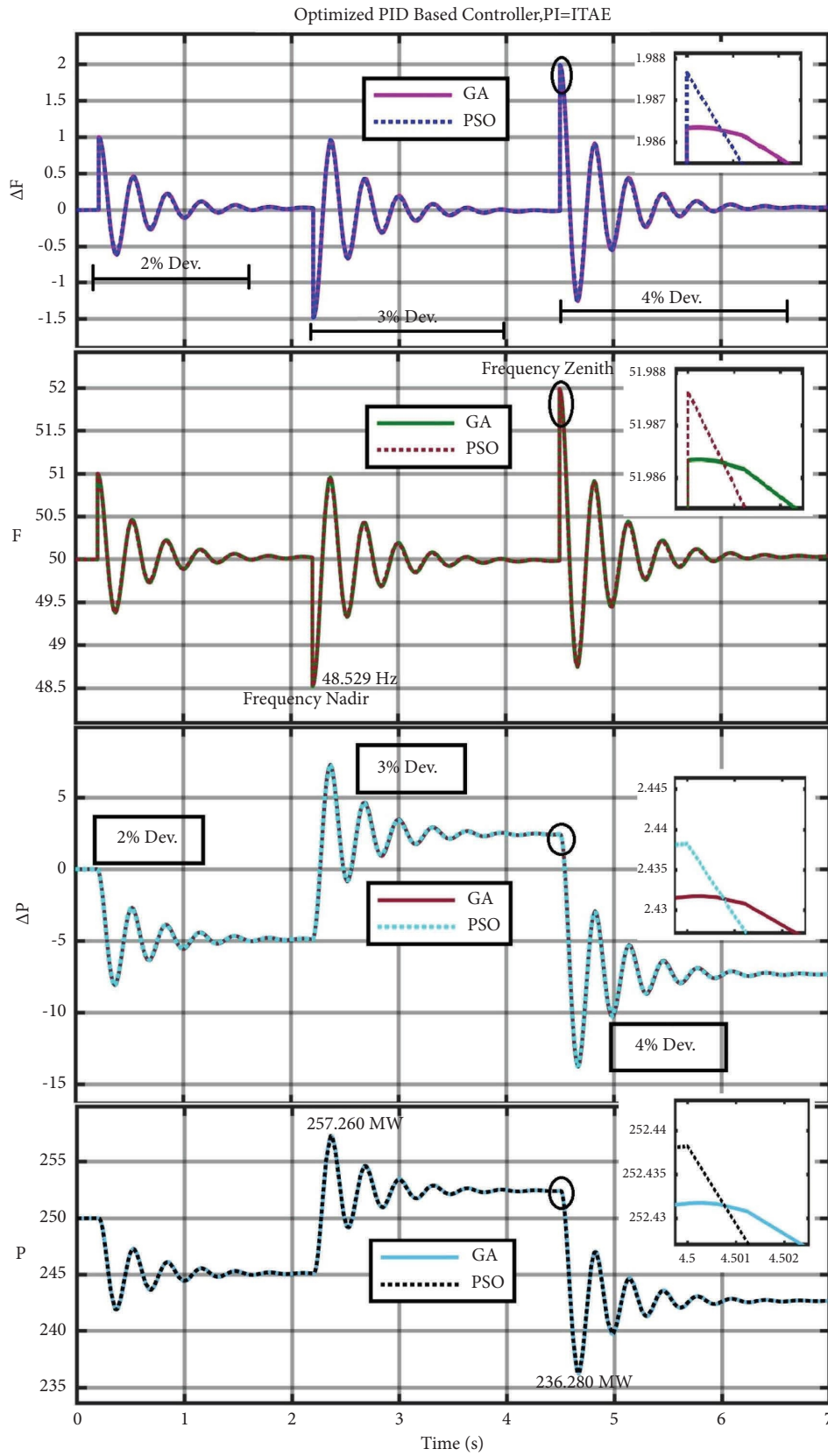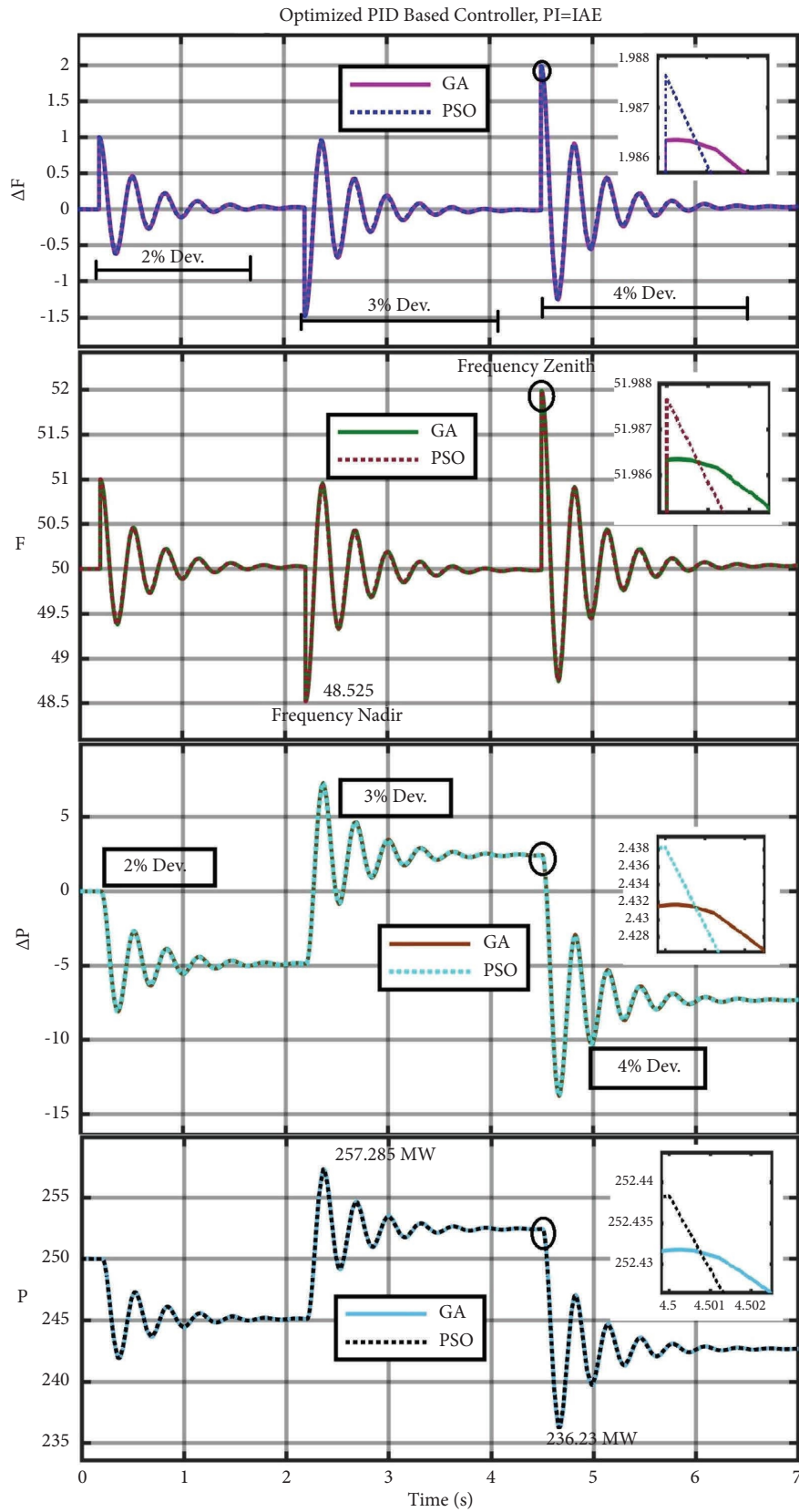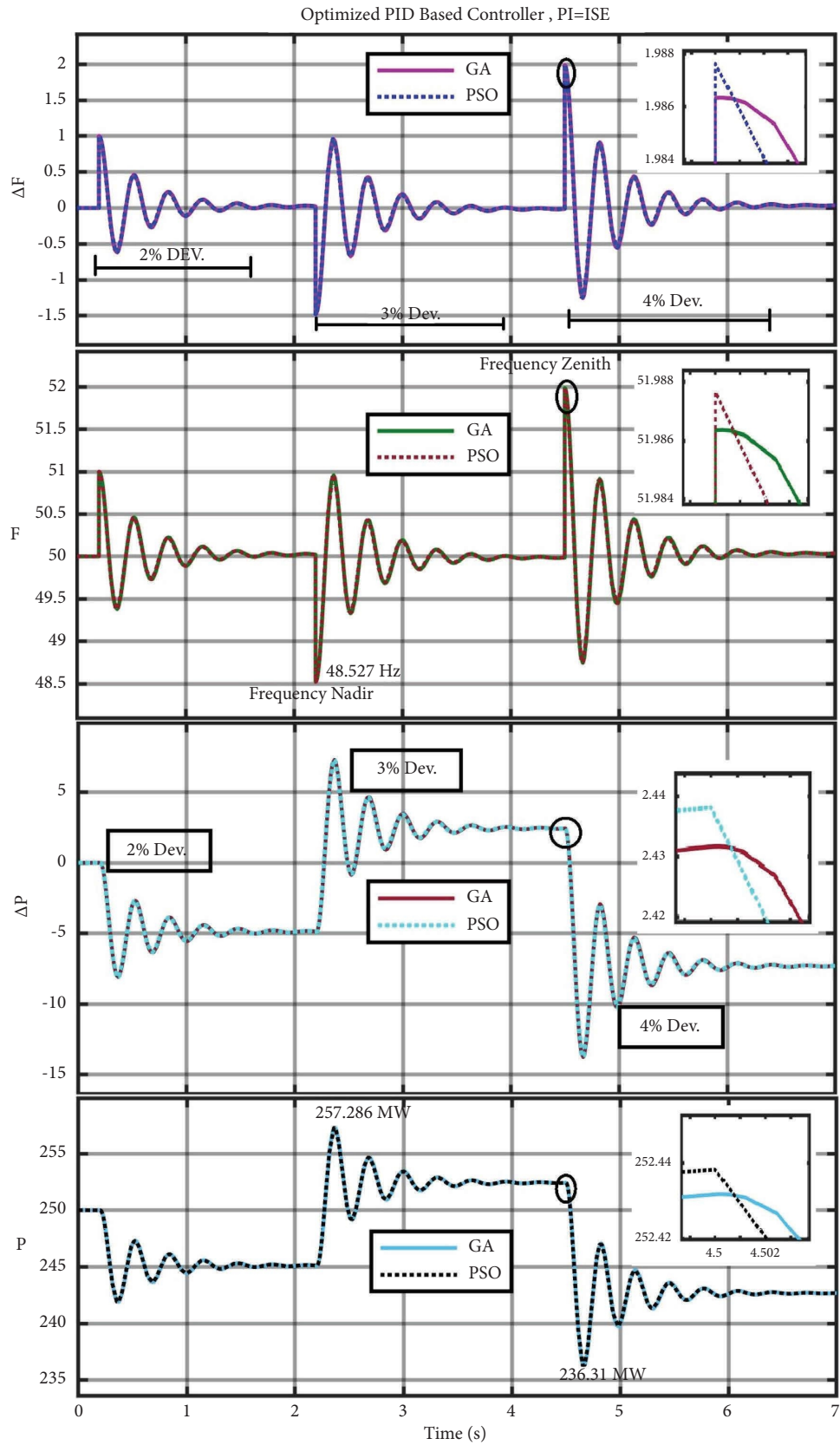
Figure 15: Response curves for change in frequency, frequency, change in power, and power optimized by improved PSO and GA-based P.I-ISE.
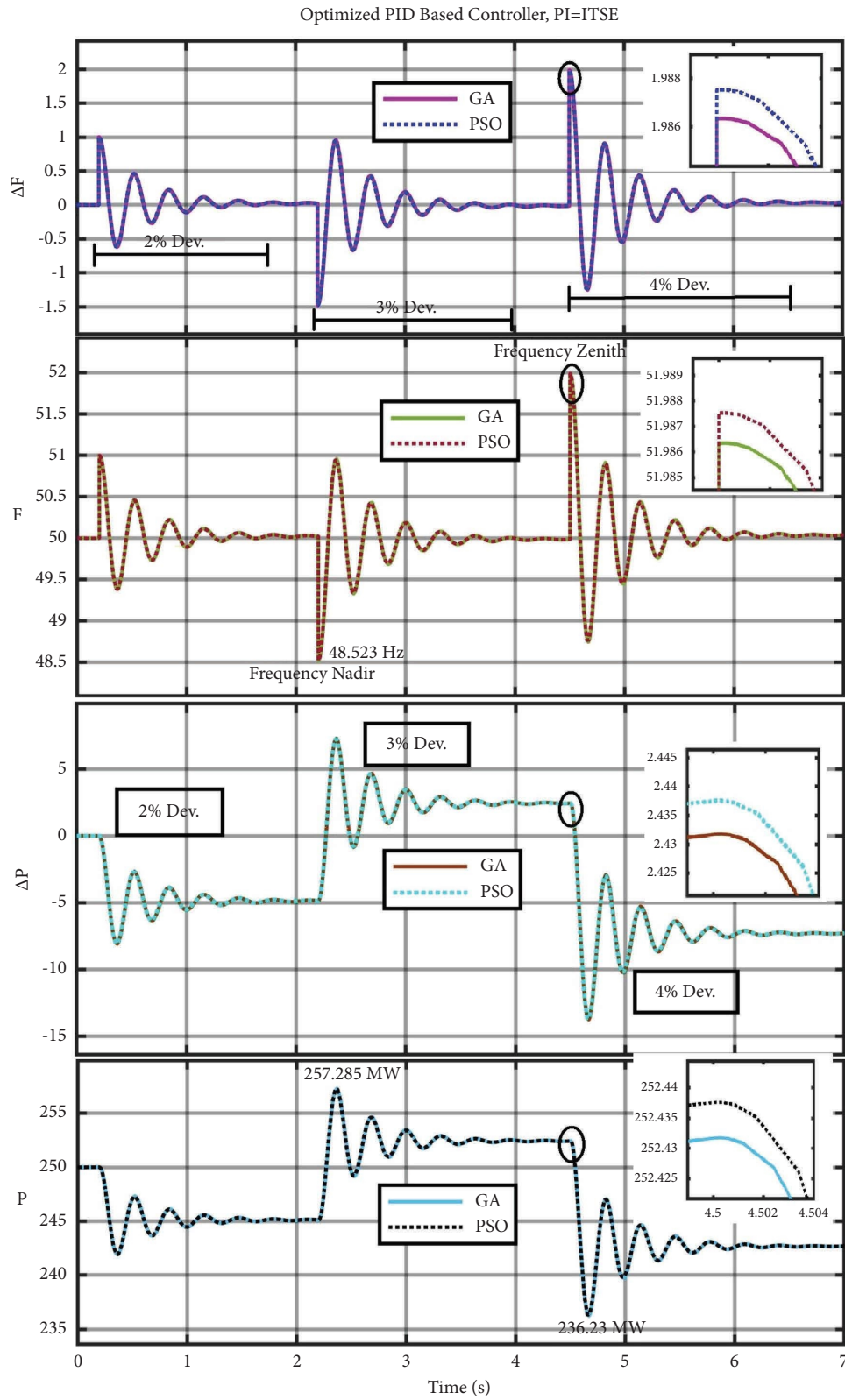
Figure 16: Response curves for change in frequency, frequency, change in power, and power optimized by improved PSO and GA-based P.I-ITSE.

TABLE 5: Statistical analysis of frequency deviation (ΔF).

PI	Type of controller	Statistical analysis of frequency deviation (ΔF)						
		Max	Min	Undershoot (%)	Overshoot (%)	Peak to peak	Mean	RMS
ITAE	PSO-PID	1.988	−1.477	−50.890	50.890	3.465	0.1721	0.8790
	GA-PID	1.983	−1.471	−50.967	50.967	3.454	0.1225	0.7492
IAE	PSO-PID	1.988	−1.478	−96.884	106.123	3.466	0.04730	0.5145
	GA-PID	1.985	−1.475	−50.953	50.953	3.460	0.1683	0.8919
ISE	PSO-PID	1.988	−1.478	−96.848	106.655	3.465	0.04846	0.4821
	GA-PID	1.983	−1.473	−50.980	50.980	3.456	0.1399	0.8155
ITSE	PSO-PID	1.988	−1.477	−50.890	50.890	3.465	0.1728	0.8888
	GA-PID	1.987	−1.477	−50.898	50.898	3.464	0.1804	0.9006

TABLE 6: Statistical analysis of power change (ΔP).

PI	Type of controller	Statistical analysis of power change (ΔP)							
		Max (MW)	Min (MW)	Rise time (ms)	Fall time (ms)	Undershoot (%)	Overshoot (%)	Peak to peak	Mean	RMS
ITAE	PSO	7.188	−13.66	57.047	48.156	10.062	64.286	20.85	−2.505	4.915
	GA	7.260	−13.72	57.881	48.663	6.212	64.286	20.98	−2.536	4.988
IAE	PSO	7.198	−13.66	56.941	47.898	10.029	64.286	20.85	−2.475	4.898
	GA	7.285	−13.77	57.595	47.331	−2.243	69.118	21.06	−2.570	5.008
ISE	PSO	7.286	−13.69	58.979	47.216	12.148	67.143	20.98	−2.450	4.882
	GA	7.199	−13.63	60.128	49.269	6.928	62.500	20.82	−2.502	4.971
ITSE	PSO	7.198	−13.66	56.941	47.898	10.029	64.286	20.85	−2.475	4.898
	GA	7.285	−13.77	57.595	47.331	−2.243	69.118	21.06	−2.570	5.008

(a)   (b)

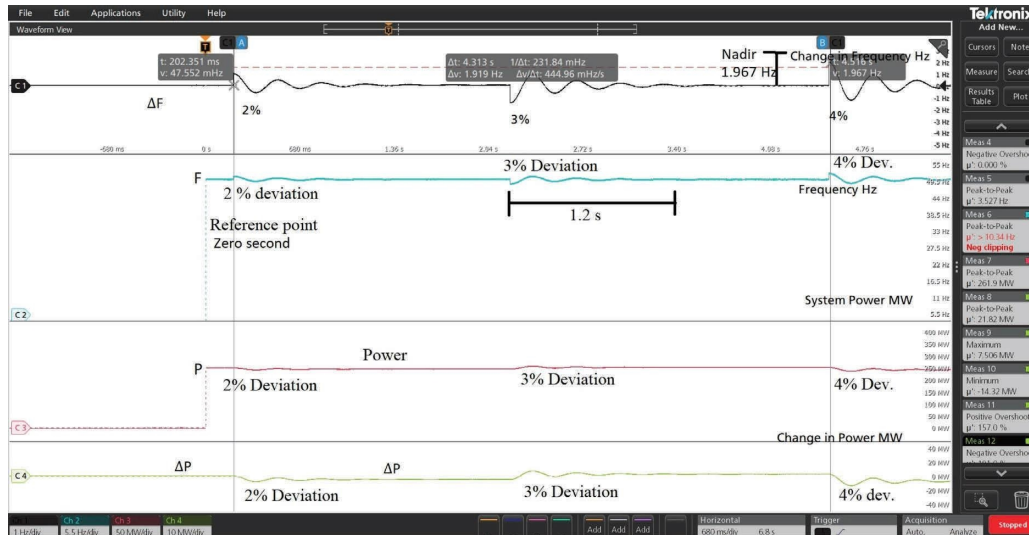FIGURE 17: Experimental hardware. (a) Setup. (b) Battery.

FIGURE 18: Experimental results for frequency deviation, frequency, power, and power change in mixed signal oscilloscope (MSO).

The simulation results for all the performance indices are shown separately in Figures 13–16. Figure 13 shows the simulation for performance index ITAE, Figure 14 presents the results for IAE, Figure 15 shows the simulation results for ISE, and in Figure 16, the simulation results for ITSE are presented. Here, each of the diagram consists of the traces of change in frequency (ΔF), frequency (F), power (P), and change of power (ΔP) for the PID optimized through PSO and GA. Here, it can be easily visualised that the GA performs better in terms of lower peak overshoot while the PSO outperforms GA in terms of settling time. Here, it is worthwhile to mention that in both the cases, the system works satisfactorily and stabilises rapidly when subject to any kind of disturbance.

Table 5 shows the statistical analysis of the changes in frequency captured in Figures 13–16.

In Table 6, power change analysis is done; it gives in-depth understanding of how this controller is very effective.

As observed in Table 5, improvised PSO PID controller has the highest overshoot as it is with all the four performance indices but restricted to the threshold of 3%. However, in all cases, it took the shortest time to settle down. On the other hand, GA PID controller has small overshoot but long settling time.

5. Experimental Results and Discussion

Simulation was done on MATLAB/Simulink environment as discussed and results were shown. Furthermore, a real-time hardware prototype was designed based on OPAL-RT (OP-4510) as shown in Figure 17. This further illustrates the efficacy of the research concept in this paper.

It is seen that the proposed dynamic controller has quick dynamic response as it takes less than two seconds to arrest any deviation despite the intensity of the change. From the experiment, 2%, 3%, and 4% disturbances were used and the response time in all the 3 cases was found to be fast.

MATLAB simulation results and experimental results from real-time OPAL-RT are in agreement giving a clear indication that the tuned optimal values of PID controller can be used in the offline system. The outcome of both the approaches is more or less similar. In Figure 18, frequency nadir is 1.967 Hz, and in MATLAB simulations as seen in Table 5, the average for all the four performance indices is 1.985 Hz. This is to validate the proposed control approach where the simulation results are almost emulated using hardware in loop.

Finally, comparisons were made between this proposed technique and some existing techniques as shown in Table 7 to ensure its effectiveness.

TABLE 7: Additional comparison between the existing control techniques from the pool of literature and the proposed control technique.

Reference	Type of control	Merits	Demerits
[36]	Droop control and VSG are proposed	It is easy to implement with low cost	Complexity in tuning parameters
[37]	Derivative control-based virtual inertia	It reduces overshoot response	Complex tuning due to trial-and-error method
[38]	Adaptive dynamics programming	Faster frequency response and reduced overshoot in d-axis	It ignores the q-axis making it incomplete due to reactive component
[39]	PID controller based (GWO)	Frequency control in multi-source single area	It did not include multiple areas and may not be applicable in microgrid
[40]	BFOA-tuned LQR-based VSG	Suppresses frequency fluctuations	Damping oscillations and RoCoF are not considered
Proposed	MPSO-based adaptive virtual inertia control	Faster frequency response with reduced overshoot and settling time and simple parameter tuning	

6. Conclusion

The designed test system based on two optimization techniques has been successfully implemented in MATLAB/Simulink. The gains obtained through these optimization methods have been further utilised for the tuning of PID regulator which further exhibits the emulation of virtual inertia control. The three different uncertainty levels caused by either intermittent RES or fluctuating load have been demonstrated to show the effectiveness of the proposed control approach. The problems of high RoCoF, high overshoot, high undershoot, and long rise time have been significantly eliminated.

The proposed techniques are suitable for regulating both RoCoF and frequency control. The above analysis confirmed that the inclusion of optimization techniques in the microgrid would act as a game changer to elusive inertia and damping. With the continuous penetration of RES/DG into our power system network, this technique will enable system control engineers to achieve steady-state operation of the overall system.

As already discussed in results section, the proposed controller's performance is tested and validated through the MATLAB simulation and hardware prototype, and the controller responds fast to the given changes. From the experimental validation, the proposed controller with excellent outcome can be used in microgrid with nonlinear loads and power supply. This adaptive virtual inertia method using optimization techniques improves frequency response and thus confirms the effectiveness of this controller.

Data Availability

The data used to support the findings of this study are included within the article.

Conflicts of Interest

The authors declare that they have no conflicts of interest.

References

[1] M. Soshinskaya, W. H. Crijns-Graus, J. M. Guerrero, and J. C. Vasquez, "Microgrids: experiences, barriers and success factors," *Renewable and Sustainable Energy Reviews*, vol. 40, pp. 659–672, 2014.

[2] J. Fang, H. Li, Y. Tang, and F. Blaabjerg, "On the inertia of future more-electronics power systems," *IEEE Journal of Emerging and Selected Topics in Power Electronics*, vol. 7, no. 4, pp. 2130–2146, Dec 2019.

[3] K. Liu, Y. Qu, H. M. Kim, and H. Song, "Avoiding frequency second dip in power unreserved control during wind power rotational speed recovery," *IEEE Transactions on Power Systems*, vol. 33, no. 3, pp. 3097–3106, May 2018.

[4] G. Delille, B. Francois, and G. Malarange, "Dynamic frequency control support by energy storage to reduce the impact of wind and solar generation on isolated power system's inertia," *IEEE Transactions on Sustainable Energy*, vol. 3, no. 4, pp. 931–939, Oct 2012.

[5] F. Blaabjerg, R. Teodorescu, M. Liserre, and A. Timbus, "Overview of control and grid synchronization for distributed power generation systems," *IEEE Transactions on Industrial Electronics*, vol. 53, no. 5, pp. 1398–1409, Oct 2006.

[6] M. M. A. H. K. Mohsen Rahimi, "Performance enhancement of parallel-operated inverter-based virtual synchronous generators supplying active load," *IET Electric Power Applications*, vol. 17, pp. 1–20, 2023.

[7] S. Maleki, J. Nikoukar, and M. H. Tousifian, "Robust Frequency Control of Microgrids: a Mixed Virtual Inertia Emulation," *International Transactions on Electrical Energy Systems*, vol. 2023, Article ID 6872765, 14 pages, 2023.

[8] N. Hatziargyriou, *Contribution to bulk system control and stability by distributed energy resources connected at distribution network*, IEEE Power Energy Soc, Piscataway, NJ, USA, 2017.

[9] H. S. A. R. M. A. M. R. H. H. Golpîra, H. Seifi, A. R. Messina, and M. R. Haghifam, "Maximum penetration level of microgrids in large-scale power systems: frequency stability viewpoint," *IEEE Transactions on Power Systems*, vol. 31, no. 6, pp. 5163–5171, Nov 2016.

[10] P. Ferraro, E. Crisostomi, M. Raugi, and F. Milano, "Analysis of the impact of microgrid penetration on power system dynamics," *IEEE Transactions on Power Systems*, vol. 32, no. 5, pp. 4101–4109, sep. 2017.

[11] J. Varela, N. Hatziargyriou, L. J. Puglisi, M. Rossi, A. Abart, and B. Bletterie, "The IGREENGrid project: increasing hosting capacity in distribution grids," *IEEE Power and Energy Magazine*, vol. 15, no. 3, pp. 30–40, 2017.

[12] G. Pandove and M. Singh, "Robust repetitive control design for a three-phase four wire shunt active power filter," *IEEE Transactions on Industrial Informatics*, vol. 15, no. 5, pp. 2810–2818, May 2019.

[13] M. K. P. S. Mandis N, "Management of low- and high-frequency power components in demand-generation fluctuations of a DFIG-based wind-dominated RAPS system using hybrid energy storage," *IEEE Transactions on Industry Applications*, vol. 50, pp. 2258–2268, 2014.

[14] X. L. J. R. J. M. G. K. T. C. Bo Long, "Frequency stability enhancement of an islanded microgrid: a fractional-order virtual synchronous generator," *International Journal of Electrical Power and Energy Systems*, vol. 147, 2023.

[15] S. Stephan, "Load frequency control of hybrid hydro systems using tuned PID controller and fuzzy logic controller," *International Journal of Engineering Research and Development*, vol. 5, March 2016.

[16] A. A. M. V. Waleed Khaled, "Fuzzy fractional-order PID control for PMSG BasedWind energy conversion system with sparse matrix converter topology," *International Transactions on Electrical Energy Systems*, vol. 2022, Article ID 3663237, p. 18, 2022.

[17] L. S. M. P. Nikhil Paliwal, "Application of grey wolf optimization algorithm for load frequency control in multi-source single area power system," *Evolutionary Intelligence*, vol. 10, 2020.

[18] K. S. Parmar, S. Majhi, and D. Kothari, "LFC of an interconnected power system with multi-source power generation in deregulated power environment," *International Journal of Electrical Power & Energy Systems*, vol. 57, pp. 277–286, 2014.

[19] G. S. da Silva, E. J. de Oliveira, L. W. de Oliveira, A. N. de Paula, J. S. Ferreira, and L. M. Honório, "Load frequency control and tie-line damping via virtual synchronous generator," *International Journal of Electrical Power & Energy Systems*, vol. 132, Article ID 107108, 2021.

[20] G. Song, X. Liu, J. Tian, and P. Wang, "An improved fuzzy voltage compensation control strategy for parallel inverter,"

International Transactions on Electrical Energy Systems, vol. 2022, Article ID 5185028, 20 pages, 2022.

[21] J. Z. L. M. K. Q. Z. G. Jianfeng Fang, "An improved virtual synchronous generator power control strategy considering time-varying characteristics of SOC," *International Journal of Electrical Power and Energy Systems*, vol. 144, 2023.

[22] B. He, Y. Ren, Y. Xue, C. Fang, Z. Hu, and X. Dong, "Research on the frequency regulation strategy of large-scale Battery energy storage in the power grid system," *International Transactions on Electrical Energy Systems*, vol. 2022, Article ID 4611426, 13 pages, 2022.

[23] J. N. H. T. Shahryar Maleki, "Robust frequency control of microgrids: a mixed H2/H∞ virtual inertia emulation," *International Transactions on Electrical Energy Systems*, vol. 2023, Article ID 6872765, p. 14, 2023.

[24] M. A. Arasomwan and A. O. Adewumi, "On the performance of linear decreasing inertia weight particle swarm optimization for global optimization," *The Scientific World Journal*, vol. 2013, Article ID 860289, 12 pages, 2013.

[25] S. Oladipo, Y. Sun, and O. Adeleke, "An improved particle swarm optimization and adaptive neuro-fuzzy inference system for predicting the energy consumption of university residence," *International Transactions on Electrical Energy Systems*, vol. 2023, Article ID 8508800, 16 pages, 2023.

[26] T. Wen, "Tuning of PID load frequency controller for power system," *Energy Conversion and Management*, vol. 50, pp. 1465–1472, 2009.

[27] H. Sadat, *Power System Analysis*, McGraw-Hill, New York, NY, USA, 1999.

[28] R. E. J. Kennedy, "Particle swarm optimization," in *Proceedings of the IEEE International Conference on Neural Network*, pp. 1942–1948, Orlando, FL, USA, June 1995.

[29] Z.-L. Gaing, "A particle swarm optimization approach for optimum design of PID controller in AVR system," *IEEE Transactions on Energy Conversion*, vol. 19, no. 2, pp. 384–391, 2004.

[30] H. Bevrani, F. Habibi, P. Babahajyani, M. Watanabe, and Y. Mitani, "Intelligent frequency control in an AC microgrid: online PSO-based fuzzy tuning approach," *IEEE Transactions on Smart Grid*, vol. 3, no. 4, pp. 1935–1944, 2012.

[31] X. H. J. M. Guimin Chen, "Natural exponential inertia weight strategy in particle swarm optimization," *Congress on Intelligent Control and Automation*, vol. 1, pp. 3672–3675, 2006.

[32] K. C. Rajasi Mandal, "Virtual inertia emulation and RoCoF control of a microgrid with high renewable power penetration," *Electric Power Systems Research*, vol. 194, pp. 1–11, 2021.

[33] A. Jayachitra and R. Vinodha, "Genetic algorithm based PID controller tuning approach for continuous stirred tank reactor," *Advances in Artificial Intelligence*, vol. 2014, Article ID 791230, 8 pages, 2014.

[34] T. Kerdphol, M. Watanabe, K. Hongesombut, and Y. Mitani, "Self-adaptive virtual inertia control-based fuzzy logic to improve frequency stability of microgrid with high renewable penetration," *IEEE Access*, vol. 7, pp. 76071–76083, 2019.

[35] S. Vachirasricirikul and I. Ngamroo, "Robust LFC in a smart grid with wind power penetration by coordinated V2G control and frequency controller," *IEEE Transactions on Smart Grid*, vol. 5, no. 1, pp. 371–380, 2014.

[36] C. L. C. Z. Yuan, C. Liu, X. Zhang, T. Zhao, X. Xiao, and N. Tang, "Comparison of dynamic characteristics between virtual synchronous machines adopting different active power droop controls," *Journal of Power Electronics*, vol. 17, no. 3, pp. 766–776, 2017.

[37] E. Rakhshani, D. Remon, A. Mir Cantarellas, and P. Rodriguez, "Analysis of derivative control based virtual inertia in multi-area high-voltage direct current interconnected power systems," *IET Generation, Transmission & Distribution*, vol. 10, no. 6, pp. 1458–1469, 2016.

[38] D. S. N. T. Naresh Malla, "Supplementary control for virtual synchronous machine based on adaptive dynamic programming," in *Proceedings of the IEEE Congress on Evolutionary Computation*, Vancouver, Canada, July 2016.

[39] L. S. P. Nikhil Paliwal, "Application of grey wolf optimization algorithm for load frequency control in multi-source single area power system," *Evolutionary Intelligence*, vol. 12.

[40] S. K. Singh, R. Singh, H. Ashfaq, and R. Kumar, "Virtual inertia emulation of inverter interfaced distributed generation (IIDG) for dynamic frequency stability & damping enhancement through BFOA tuned optimal controller," *Arabian Journal for Science and Engineering*, vol. 47, no. 3, pp. 3293–3310, 2021.